35th Annual International Conference of the IEEE EMBS
Osaka, Japan, 3 - 7 July, 2013

Boundary Condition Generating Large Strain on Breast Tumor for Nonlinear Elasticity Estimation

Mariko Tsukune, Maya Hatano, Yo Kobayashi, Tomoyuki Miyashita, M. G. Fujie, *Fellow, IEEE*

***Abstract*—We describe a robotic palpation system that determines whether a breast tumor is benign or malignant by measuring its nonlinear elasticity. Two indenters compress the breast from different directions to generate sufficient strain on the inner tumor, which simply represents clinical dynamic testing. The nonlinear elasticity of the inner tumor is estimated by correcting the reaction force data of the surrounding soft tissue. Here, we present the basic concept of our study and simulation results considering geometric conditions of the indenters using a finite element breast model. Indenters with variable width are applied to the breast at several contact positions in a simulation for comparison. Our results indicate that when the spring stiffness between the contact position of one indenter and the center of the tumor equals the spring stiffness between the contact position of the other indenter and the center of the tumor, a larger contact area (i.e., larger spring stiffness) provides larger strain acting on the inner tumor.**

I. Introduction

In recent years, early detection of breast cancer has been possible because of advances in imaging technology. However, it is difficult to make a definite diagnosis using palpation or imaging modalities, and invasive examinations such as biopsy are needed to determine whether a breast tumor is benign or malignant. Therefore, accurate non-invasive diagnostic methods are required for accurate diagnosis and to alleviate the pain felt by and the mental burden placed on patients.

The elasticity of a suspicious tumor has traditionally been qualitatively measured through palpation by doctors. In particular, elastography imaging technologies have attracted consideration. In elastography, an external force induces strain on the suspicious tumor and the subsequent deformation is measured by conventional medical imaging modalities, from which mechanical properties can be reconstructed.

The focus of elastography techniques had typically been on the imaging contrast in linear elasticity, but attention has shifted toward nonlinear elasticity in recent years. Krouskop et al. [1], Wellman et al. [2], and Samani et al. [3] measured the stiffness properties of breast tissues and reported that breast tissues under low strain exhibit linear properties, while stiffness increases nonlinearity under high strain. Furthermore, they indicated that the difference between a benign tumor and a malignant tumor is greater in terms of the nonlinear property than in terms of the linear property. Therefore, it is necessary to measure the nonlinear elasticity of a suspicious tumor under high strain to determine whether the tumor is benign or malignant.

The goal of this study is to develop a robotic palpation system to determine whether a breast tumor is benign or malignant by measuring its nonlinear elasticity. Figure 1 describes the schema of our palpation system. We have previously reported that the reaction force data of the surrounding soft tissue can indicate the nonlinear property of the inner tumor when a tumor is deformed sufficiently. Therefore, using our system, external forces are applied to the soft tissue by two indenters to generate sufficient strain on the inner tumor. Placements of the indenters are simply modeled on clinical dynamic testing. Dynamic testing is a manual technique for ultrasonic diagnosis to examine deformability of the tumor. The ultrasonologist grasps the patient's breast with the thumb and the other fingers of one hand to apply external forces from two different directions, and examines the deformation of the tumor manipulating an ultrasonic probe with the other hand. Two indenters of our palpation system represent the thumb and the other fingers of the ultrasonologist respectively. The strain magnitude of the tumor depends on the contact positions, the contact areas and the directions of the fingers, which are represented as those of indenter movements in our palpation system. Therefore, we evaluated the effect of the geometric conditions of indenters.

Some researchers have focused on generating sufficient strain on an inner tumor of soft tissue. Shiina et al. [4], [5] and Wang [6] applied external compression on the target tissue using two boards. Kim et al. [7] examined the surface deformation and force response of soft tissue depending on various indentation depths and different tip shapes. Barbone et al. [8] considered the boundary conditions that can and cannot

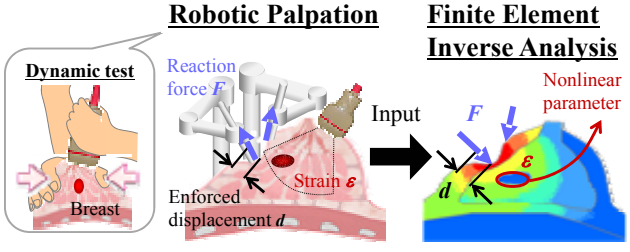

Figure 1. Schematic diagram of our robotic palpation system.

Manuscript received February 4th, 2013. This work was supported in part by the Global COE Program "Global Robot Academia" of MEXT (Ministry of Education, Culture, Sports, Science and Technology of Japan), the High-Tech Research Center Project of MEXT, a Grant-in-Aid of Scientific Research from MEXT (nos. 22360108 & 22103512), a Waseda University Grant for Special Research Projects (no. 2010B-177), and the Cooperative Research Project of the Institute of Development, Aging and Cancer, Tohoku University.

M. Tsukune, M. Hatano are Members of the Graduate School of Science and Engineering, Waseda University, Japan (59-309, 3-4-1, Okubo, Shinjuku Ward, Tokyo, Japan. E-mail: mtsukune@moegi.waseda.jp; Tel: +81-3-5286-3412; Fax: +81-3-5291-8269).

Y. Kobayashi, T. Miyashita, and M. G. Fujie are Members of the Faculty of Science and Engineering, Waseda University, Japan.

be inferred from strain images. However, these papers did not clarify the relationship between the geometric boundary conditions and the strain on the inner tumor.

The objective of the present paper is to evaluate the geometric effect of two indenters on the strain magnitude of the inner tumor. In this paper, we focus on the contact positions and contact areas of two indenters. Simulation analysis for several contact positions and contact areas using a finite-element breast model was performed to clarify the relationship between the geometric boundary conditions and the strain on the inner tumor.

II. METHOD

To derive the optimal contact positions and contact areas that generate sufficient strain on the inner tumor of soft tissue, we evaluated the strain magnitude of the tumor for several contact positions by simulation using a finite-element breast model. The contact positions defined by the compression angles and contact areas of each indenter were set variants for comparison.

A. Nonlinear Elastic Model

We have previously reported a nonlinear elastic model of a hog liver and breast [9]. This model was constructed using torsional creep. In our previous work, the nonlinear properties were modeled using the quadratic function of strain described in (1).

$$E = \begin{cases} E_o & (\varepsilon < \varepsilon_0) \\ E_0(1 + a_\varepsilon(\varepsilon - \varepsilon_0)^2) & (\varepsilon > \varepsilon_0) \end{cases}, \quad (1)$$

where E is the magnitude of the stiffness, E_0 is the elastic modulus of the linear range, a_ε is a coefficient representing the increasing level of elasticity when a change in the tumor-type tissue appears in the nonlinear deformation data, ε is the strain and ε_0 is the strain in which the characteristics of soft-tissue change show nonlinearity.

B. Finite Element Modeling

We have previously reported our solution for the finite element model and have also provided specific descriptions of the development of this model [9]. This model has two types of nonlinear elastic parameters, for the normal breast and for the mock tumor, because these target objects are reproducible in an in vitro experiment. As shown in Fig. 2, the shape of the breast model was assumed to be a semi-ellipse, which was 100 mm in diameter and 40 mm in height. The shape of the tumor field was assumed to be a circle, 10 mm in diameter. The x-coordinate of the tumor's center was 20 mm, and the y-coordinate was the middle of the breast's height, as shown in Fig. 2. As an initial boundary condition, we set the dorsal side of the model to be the fixed end, simulating the effect of the sternum. The mesh was developed using the Delaunay method, which involves automatically dividing the object into triangular elements, according to the outline of the target object. The mesh was created to form three types of circle: one with a diameter of 12 mm that circumscribed all the individual triangular finite elements of the mesh, one with a diameter of 0.6 mm that circumscribed all of the elements existing within a radius of 8 mm from the points at which the indenters make contact and the points of the above circular profile of the tumor, and one with a diameter of 0.4 mm that circumscribed all of the elements existing within a radius of 8 mm from the tumor's center point.

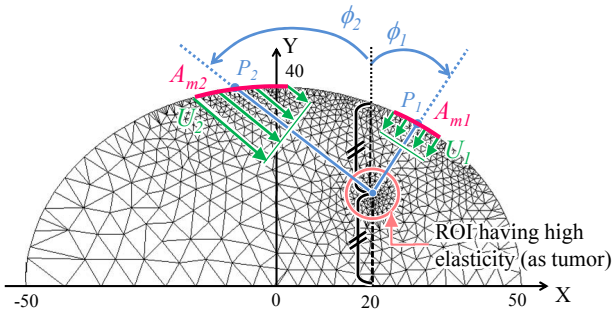

Figure 2. Shape and mesh of the breast model. The number of elements was 1616, and the number of nodes was 906.

TABLE I. Nonlinear elastic parameters.

Type	Normal breast		Malignant tumor	
	Ratio	Value	Ratio	Value
Elastic modulus E_0 kPa	1.00	14.4	2.63	37.9
Coefficient a_ε	1.00	93.0	3.17	295
Limitans Strain ε_0	1.00	0.087	1.03	0.0896

C. Material Parameters

The stiffness parameter of the model was decided according to our previous work in measuring the nonlinear elasticity of breast tissues [10]–[12]. Table I gives the parameters of the normal breast tissue and the malignant tumor.

D. Simulation Conditions

To determine the optimal contact positions and contact areas of each indenter, we defined the three following variables for comparison. We conducted simulations under several conditions of the variables in the simulation.

1) Indenter Angle ϕ: Setting the contact points closer to the target tumor can expand the stress distribution and generate larger strain on the target. The defined domain of the contact points was limited to the semicircular profile of the soft tissue. The contact point P is described as the angle of the direction from P to the center of the target C with respect to the y-coordinate. An indenter was set at the angle of degree. We selected contact positions of 30, 45, 60 and 90 degrees in our simulation analysis; the lengths between the contact point P and the center of the target C are given in Table II.

TABLE II. Length between the contact point and the center of the target.

Length mm	Indenter Angles ϕ deg.			
	30	45	60	90
P_1C	16.83	17.31	18.63	24.44
P_2C	24.46	30.61	39.88	64.44

2) *Contact Area A :* We previously reported that the range of a stress distribution depends on the shape and size of the manipulator tip [13]. A larger contact area can generate larger strain acting on both the target tumor and the surrounding tissue. The contact area is described as the width of the tip of each indenter since a flat tip was applied for simplification in finite element analysis. We selected widths of 5, 10, 15 and 20mm, where the ratio of the width to diameter of the tumor was 1/2, 1, 3/2 and 2 in this paper.

3) Enforced displacement d : The enforced displacement d was set the same for the two indenters, with values ranging from 0 to 20 mm at 0.4-mm intervals.

E. Strain Magnitude

To find the optimal conditions for generating sufficient strain on the inner tumor, we define an evaluation value. A larger displacement magnitude generates larger strain acting on the target tumor although it simultaneously generates large strain acting on the surrounding tissue. However, excessive compression causes pain in the breast. We define the lower limit of strain acting on the inner tumor. Additionally, we define the evaluation value f as the compression displacement when the average of the von Mises strain $\bar{\varepsilon}_{ROI}$ acting on the inner tumor given by Eq. (1) exceeds the lower limit. Equation (2) expresses the evaluation value.

We set the lower limit of the average of the von Mises strain $\bar{\varepsilon}_{ROI}$ acting on the inner tumor to 0.17, which is twice the strain at which the characteristics of normal breast tissue change show nonlinearity, to ensure a sufficient difference in deformation between the normal breast and malignant tumor. In equation (1), S^e is the elemental area and ε_m is the von Mises strain.

Conditions minimizing f readily allow the generation of sufficient strain acting on the inner tumor.

$$\bar{\varepsilon}_{ROI} = \frac{\sum S^e \varepsilon_m}{\sum S^e} \qquad (1)$$

$$f = d \qquad (\bar{\varepsilon}_{ROI} = 0.17) \qquad (2)$$

III. RESULTS

We present simulation results. We focus on the ratio of length P_1C to P_2C in describing the relationships between evaluation values and contact positions and contact areas. Figure 3 shows the relationship between the evaluation value and the ratio of length P_1C to P_2C. The index of the parameter is the number of indenters. When the ratio of length P_1C to P_2C is less than 3.0, it has positive correlation with the evaluation value. When the ratio of length P_1C to P_2C is more than 3.0, it has low negative correlation with the evaluation value. The evaluation value is at a minimum when the ratio of length P_1C to P_2C is about 1.0, indenter angle ϕ_1 is 90 degrees, and indenter angle ϕ_2 is 30 degrees.

We explain separately the relationships between the evaluation value and the contact positions and contact areas using the ratio of length P_1C to P_2C. The coefficient of correlation between the evaluation value and each parameter is given in Table IV.

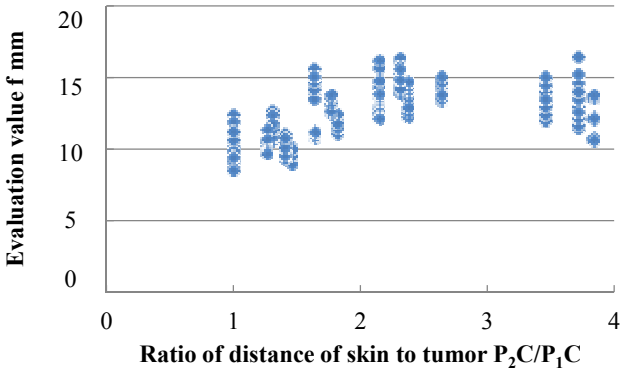

Figure 3. Relationship between the evaluation value and the ratio of length P_1C to P_2C.

TABLE IV. COEFFICIENT OF CORRELATION BETWEEN THE EVALUATION VALUE AND EACH PARAMETER

Parameter	Correlation coefficient	
	$P_2C/P_1C < 3.0$	$P_2C/P_1C \geq 3.0$
Indenter Angle ϕ_1	-0.25	0.44
Indenter Angle ϕ_2	0.63	
Contact area A_1	0.26	0.32
Contact area A_2	-0.15	0.81

A. Case that the ratio of length P_1C to P_2C is less than 3.0

The correlation between the evaluation value and the contact position differs between the indenters. In the case of indenter 1, there is poor correlation between the evaluation value and indenter angle ϕ_1. In the case of indenter 2, the evaluation value decreases as the indenter angle ϕ decreases. The evaluation value is a minimum at indenter angle $\phi_2 = 30$ degrees.

There is poor correlation between the evaluation value and contact area A for both indenters. The evaluation value is a minimum for contact area $A_1 = 15$ mm and contact area $A_2 = 20$ mm.

B. Case that the ratio of length P_1C to P_2C is more than 3.0

In the case of indenter 1, there is positive correlation between the evaluation value and indenter angle ϕ_1. The evaluation value is a minimum at indenter angle $\phi_1 = 90$ degrees. In the case of indenter 2, there is no correlation between the evaluation value and indenter angle ϕ_2 because indenter angle ϕ_2 is 90 degrees only.

In the case of indenter 1, there is poor positive correlation between the evaluation value and contact area A_1. In contrast, there is high positive correlation between the evaluation value and contact area A_2.

IV. DISCUSSION

In this section, we discuss how the geometrical condition can be used to generate sufficient strain acting on the inner tumor from simulation results.

We consider that the strain acting on the inner tumor is decided by the ratio of the spring stiffness between the contact position of one indenter and the center of the tumor to the spring stiffness between the contact position of the other indenter and the center of tumor. Figure 5 shows the deformation of the breast model when the breast model has the geometrical conditions that minimize and maximize the evaluation value. When two indenters compress the breast by the same displacement, the inner tumor moves in the direction of lower spring stiffness as seen in Fig. 5 (a). If the spring stiffnesses of the tissue between the contact position of the indenter and the center of the tumor are the same for the two indenters, the inner tumor is deformable because the inner tumor moves less, as seen in Fig. 5 (b).

Spring stiffness is inversely proportional to the length between the contact position and center of the tumor, and is proportional to the contact area. However, simulation results show that there is high correlation between the evaluation value and the ratio of length P_1C to P_2C, and there is low correlation between the evaluation value and the contact area. We consider that although the contact area and enforced displacement are the same, the strain on the inner tumor differs depending on the indenter angle because the state of contact between the indenter and breast differs depending on the indenter angle. We calculated the coefficient of correlation between the evaluation value and the contact area when the ratio of length P_1C to P_2C is 1.0; the correlation coefficient for A_1 is –0.48 and that for A_2 is –0.83. Hence, a larger contact area (i.e., larger spring stiffness) promotes the generation of large strain acting on the inner tumor.

Therefore, when the spring stiffness between the contact position of one indenter and the center of the tumor equals the spring stiffness between the contact position of the other indenter and the center of tumor, a larger contact area (i.e., larger spring stiffness) produces larger strain acting on the inner tumor.

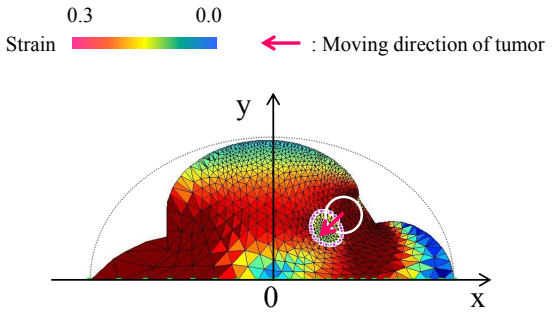

(a) $P_2C/P_1C = 3.5$ ($\phi_1 = 60$ deg., $\phi_2 = 90$ deg.)

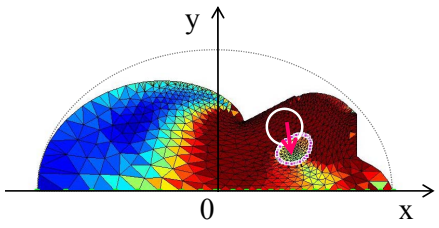

(b) $P_2C/P_1C = 1.0$ ($\phi_1 = 90$ deg., $\phi_2 = 30$ deg.)

Figure 5. Deformation of the breast model.

V. Summary

The objective of the present paper is to evaluate the geometric effect of two indenters on the strain magnitude of the inner tumor for the development of a robotic palpation system to determine whether a breast tumor is benign or malignant through measuring its nonlinear elasticity. Finite element analysis for several contact positions and contact areas was performed to clarify the relationship between the geometric conditions and the strain acting on the tumor. The simulation showed that, when the spring stiffness between the contact position of one indenter and the center of the tumor equals the spring stiffness between the contact position of the other indenter and the center of the tumor, a larger contact area (i.e., larger spring stiffness) readily promotes the generation of large strain acting on the inner tumor. In future work, we will perform simulation analysis using breast models of various shapes and various elastic properties. Additionally, we will perform *in vitro* experiments to evaluate the optimal geometry conditions derived from simulation analysis.

References

[1] T. A. Krouskop, T. M. Wheeler, F. Kallel, B. S. Garra, and T. Hall, "Elastic moduli of breast and prostate tissues under compression", *Ultrason. Imaging*, vol.20, pp.260-274, 1998.

[2] P.S. Wellman, "Breast Tissue Stiffness in Compression is Correlated to Histological Diagnosis", *Ph. D. dissertation*, Harvard University, USA, 1999.

[3] J. O' Hagan, and A. Samani, "Measurement of the hyperelastic properties of 44 pathological ex vivo breast tissue samples", *J. Phys. Med. Biol.*, vol.54, pp.2557–2569, 2009.

[4] N. Nitta and T. Shiina, "Estimation of Nonlinear Elasticity Parameter of Tissues by Ultrasound", *Jpn. J. Appl. Phys.* vol. 4, pp. 3572–3578, 2002.

[5] T. Shiina, "The quantitative assessment method of tissue elasticity distribution by ultrasonography", *Journal of the Society of Instrument and Control Engineers*, vol.45, 11 issue, pp.940-947, 2006.

[6] Z. G. Wang, Y. Liu, G. Wang, and L. Z. Sun, "Elastography Method for Reconstruction of Nonlinear Breast Tissue Properties", *International Journal of Biomedical Imaging*, Article ID 406854, 2009.

[7] B. Ahn, and J. Kim, "Measurement and characterization of soft tissue behavior with surface deformation and force response under large deformations", *Journal of the Medical Image Analysis*, vol. 14, pp. 138–148, 2010.

[8] P. E. Barbone, and J. C. Bamber," Quantitative elasticity imaging: what can and cannot be inferred from strain images", *Journal of Physics in Medicine and Biology,* vol. 47, pp.2147-2164, 2002.

[9] Y. Kobayashi, A. Onishi, T. Hoshi, K. Kawamura, M. Hashizume, M. G. Fujie, "Development and validation of a viscoelastic and nonlinear liver model for needle insertion", *J. Computer Assisted Radiology and Surgery*, vol. 4 (1), pp. 53-63, 2009.

[10] M. Tsukune, Y. Kobayashi, T. Hoshi, T. Miyashita, M. G. Fujie, "Evaluation and comparison of the nonlinear elastic properties of the soft tissues of the breast", *33st Annual International Conference of the IEEE Engineering in Medicine and Biology Society*, Boston, pp. 7405-7408, 2011.

[11] M. Tsukune, Y. Kobayashi, T. Hoshi, Y. Shiraishi, T. Yambe, T. Miyashita, and M. G. Fujie, "Nonlinear Reaction Force Analysis for Characterization of Breast Tissues", *Springer PICT*, ACCAS2011, 2012.

[12] M. Tsukune, Y. Kobayashi, T. Miyashita, and M. G. Fujie, "Breast tumor phantom utilizing heat coagulation to mimic nonlinear elasticity", *27th International congress and exhibition on Conputer Assisted Radiology and Surgery*, PO12-00050.

[13] M. Hatano, Y. Kobayashi, M. Suzuki, Y. Shiraishi, T. Yambe, M. Hashizume, and M. G. Fujie, "Geometry Effect of Preloading Probe on Accurate Needle Insertion for Breast Tumor Treatment", *2012 IEEE International Conference on Robotics and Automation*, Minnesota, pp. 1933-1938, 2012.